Droplet evaporation in the context of interstage injection

Inez von Deschwanden, Friedrich-Karl Benra, Dieter Brillert, Hans Josef Dohmen

Droplet evaporation in the context of interstage injection

Inez von Deschwanden[1]*, Friedrich- Karl Benra[1], Dieter Brillert[1], Hans Josef Dohmen[1]

ISROMAC 2016

International Symposium on Transport Phenomena and Dynamics of Rotating Machinery

Hawaii, Honolulu

April 10-15, 2016

Abstract

Wet compression is a widely used approach to maximize the power rate of stationary gas turbines. This technique is practically realized by liquid water injection into the air main flow. Water is injected via a nozzle rack at the air inlet duct of the compressor. Only minor parts of the injected water evaporate on their way to the compressor inlet. Therefore, a multi-phase flow of humid air and water droplets enters a compressor operating in wet compression mode. Water injection between compressor stages is called interstage injection. This technique is challenging and rarely investigated yet.

In this paper, a parametric study of the evaporation process with regard to the conditions of interstage injection is presented. Evaporation performance is calculated using the droplet vaporization model of Abramzon, et al. [1]. The compression process is calculated using an axial compressor model. Physical limits referring to evaporation process and internal compressor cooling are discussed. A thermodynamic analysis of interstage injection is presented with focus on the amount of water required for optimized cooling.

Keywords

droplet evaporation — interstage injection — compressor cooling

[1]*Chair of Turbomachinery, University of Duisburg-Essen, Lotharstr.1, D-47057 Duisburg, Germany, Tel: +49 (203)-379-1699, Fax: +49 (203)-379-3038*

***Corresponding author**: inez.deschwanden@uni-due.de

Introduction

Inlet air cooling is a commonly used technique to increase gas turbine power output. The increase of ambient air temperature decreases simultaneously the gas turbine power output of about 0.54 %-0.9 % per degree, Chaker, et al. [2]. There are four common evaporative inlet cooling systems:

- evaporation cooling
- inlet fogging
- wet compression
- interstage injection

The installation of the four water injection systems is schematically pictured in Fig. 1. For evaporation cooling the air mass flow is cooled while the air goes through wet gauze, placed at the entrance of the air inlet duct. In this application evaporative cooling of the air is achieved through the air contact with the wet gauze. No water is injected into the air mass flow. For inlet fogging the air mass flow is cooled by water injection into the air inlet duct until the wet bulb temperature is attained. Within this process only the water amount needed for air saturation is injected. Hence saturated air at wet bulb condition but no water droplets enters the compressor.

The third technique is wet compression. In literature this technique is also called overspray fogging. The technique of wet compression is similar to the one used for inlet fogging. The air mass flow is similarly to the inlet fogging technique cooled down by water injection into the air inlet duct of the compressor. However, the amount of injected water is higher than the amount which is injected for inlet fogging. In contrast to inlet fogging, during the wet compression process a mixture of saturated air and water droplets enters the compressor. The major advantage of the wet compression system compared to the inlet fogging is the evaporation of water droplets during the compression process.

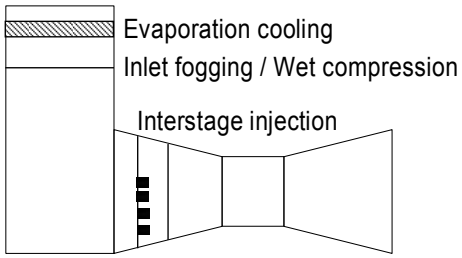

Figure 1 Evaporative cooling systems for gas turbines

The continuously cooled compression process leads to an increase of the gas turbine power output. Thermodynamic analyses of the wet compression process are given by Zheng, et al. [3], Zheng, et al. [4] and Bianchi, et al. [5]. Aerodynamic analyses of the wet compression process e.g. by Brun, et al. [6] and Sun [7] point out that there is the risk of aerodynamic instabilities for wet compression processes due to changed compressor operating conditions.

Water injection between compressor stages is called interstage injection. For wet compression systems just one or two injection points exist in the air inlet duct. Small droplets are injected because of following the compressor main flow best. The aim is to prevent that droplets hit the walls. If droplets hit walls they form a water film. The evaporation of water films performs slower than droplet evaporation process. Additionally, the evaporation time of small droplets is faster than the

evaporation time of bigger droplets. A shorter evaporation time leads to a cooling effect mainly in the first compressor stages.

Interstage injection enables a continuous water injection during the compression process. With this technique further cooling of the last compressor stages can be achieved.

Interstage injection offers the possibility for water injection at specific positions. Therefore optimized cooling can be realized during the compression process. The amount of injected water can be adapted to operating conditions. For specific operating conditions water can be injected at individual injection positions in order to improve compressor cooling. Additionally, the risk of blade icing at the first compressor stages can be avoided if water is injected between the stages and not in front of the compressor.

Injecting water between the compressor stages leads also to changed compressor operation. Comparable to wet compression there is also the risk of aerodynamic instabilities; see e.g. Brun, et al. [6]. Different methods for interstage injection exist. Wang, et al. [8] present a model for water injection between high-pressure and low-pressure compressor parts. Bagnoli, et al. [9] present an interstage injection system with eight water injection points. The first injection point is within the inlet duct to saturate the air in the inlet duct. The seven additional injection points are located between the first eight compressor stages. Further water injection between the stages leads to a supplemental evaporation during the compression process and therefore cools the air down. Other examples demonstrate water injection just in between the compressor stages; see e.g. Brun, et al. [6].

Interstage injection systems are rarely investigated yet. Bagnoli, et al. [9] and Roumeliotis, et al. [11] calculate the benefit of the interstage injection process for some operation conditions. Ingistov [12] describes a first nozzle test of an interstage injection system for online compressor washing due to water injection between the compressor stages.

In this paper a study of the evaporation of droplets in the context of interstage injection for axial compressors is presented. The evaporation performance is calculated for different initial spray conditions.

Nomenclature

B	Transfer number
C	Compression rate, s^{-1}
c_p	Specific heat capacity, J (kg K)$^{-1}$
D	Diffusion coefficient, m²s^{-1}
d	Nozzle Diameter, m
dm	Evaporated mass flow, kg s^{-1}
h	Specific enthalpy, kJ kg^{-1}
L	Latent heat of evaporation, kJ kg^{-1}
l	Characteristic length, m
$\dot{m}$	Mass flow, kg s^{-1}
n	Polytropic exponent
p	Pressure, bar
$\dot{Q}_L$	Heat transferred into droplet, kJ s^{-1}
R	Molar gas constant, J mol^{-1} K^{-1}
r	Radius, m
s	Entropy, J (kg K)$^{-1}$
T	Temperature, K
t	Time, s
u	Velocity, m s^{-1}
v	Specific volume, m³ kg^{-1}
x	Mass fraction
Y	Vapor mass concentration
z	Number, real gas factor
x	Mass fraction
α	Heat transfer coefficient, J m^{-2} K^{-1} s^{-1}
η	Efficiency
κ	Isentropic exponent
λ	Thermal conductivity, W m^{-1} K^{-1}
π	Pressure ratio
ρ	Density, kg m^{-3}
σ	Surface tension, $N\ m^{-1}$
ϕ	Non-dimensional correction parameter

Subscripts and superscripts

air	Air
d	Droplet
dry	Dry process, evaporation neglected
g	Gas film
i	Time step, initial
L	Liquid
M	Mass
poly	Polytropic
rel	Relative
S	Surface
T	Heat
vap	Vapour
w	Water
*	Modified value
0	Initial state, without Stefan flow
¯	Average value
∞	Far from droplet

Non-dimensional numbers

C_D	Drag coefficient
Le	Lewis-number, $\frac{Sc}{Pr}$
Nu	Nusselt-number, $Nu = \frac{\alpha\, l}{\lambda}$
Pr	Prandtl-number, $\frac{\eta}{\lambda / c_p}$
Re	Reynolds-number, $\frac{\rho\, u\, l}{\eta}$
Sc	Schmidt-number, $\frac{\eta}{\rho\, D}$
Sh	Sherwood-number, $Sh = \frac{g\, l}{\rho\, D}$
We	Weber-number, $We = \frac{\rho\, l\, \Delta u^2}{\sigma}$

1. Methods

Water injection between compressor stages is technically challenging. Nozzles are required to inject the water between the compressor stages. The influence of the water injection on the compressor flow should be minimized. Therefore is it essential to have nozzles producing a fine widely dispersed water spray. The spray should be homogeneous and consisting of tiny droplets with a diameter of less than 10 µm, see e.g. Schnitzler, et al. [13]. Tiny droplets are required because they follow the compressor flow best. The short relaxing time of those tiny droplets reduces blade erosion due to avoiding the impact of droplets on the blades.

The residence time of water droplets inside the compressor is very short, in the range of 15 ms-30 ms. Thus, high

evaporation rates are needed for the evaporative cooling process. The evaporation rates increase significantly when the droplet diameter is decreased. Nevertheless might the evaporation process of droplets with a diameter of 10 µm be even too slow for their overall residence time in a compressor.

An increase of the temperature of the injected water has the effect that water surface tension is reduced. This reduction leads to a higher Weber-number. Spray generation at higher Weber-numbers results in reduced droplet diameter for the same nozzle hardware. A reduced droplet diameter enables the injection of higher water mass fractions due to the faster evaporation of smaller droplets. Therefore the injection even of higher water mass fractions with its consequence on the evaporation performance during the compression process is analyzed. This analyzation enables the estimation of the potential of interstage injection in axial compressors. The droplet evaporation model by Abramzon, et al. [14] is used to calculate the droplet evaporation. An influencing factor for the evaporation performance is the relative velocity between droplet and gas phase. The strength of this factor for the actual calculations is therefore firstly determined. The dependence of the droplets diameter on its ability to follow the main flow is investigated. In the second step is the dependence of the evaporation on the droplet temperature established. Finally the calculation of the evaporation ability at compressor conditions needs to be modeled.

2. Calculation model

The evaluation of the droplet evaporation in this paper consists of a heat- and mass-transfer model for the droplet evaporation determination and a model for the compression process. There are different methods for calculating the effect of evaporative cooling. White, et al. [15] uses a 1D-approach to calculate the evaporation effect on the compressor performance. He assumes that entropie change due to aerodynamic effects can be neglected

$$T\,ds = dh - v\,dp \tag{1}$$

For ideal gas and ideal mixture leads Eq. 1 to

$$c_p^* \frac{dT}{T} = R^* \frac{dp}{p} \tag{2}$$

with c_p^* and R^* as the specific heat and gas constant for the air-vapor and water mixture. For further information see White, et al. [15]. This assumption is also used by Young [16]. Härtel, et al. [17] calculates the effect of the wet compression process on compressor performance with two models. The first model is an ideal model, which predicts fast evaporation with saturated air at any time. The second model is a droplet evaporation model which also assumes permanently saturated air. Their results fit well for a droplet diameter of 1 µm. But for droplet diameters bigger than 1 µm the evaporation process performance slows down. Due to the slower evaporation process it is impossible to get a continuous saturation of the air. This leads to a minor temperature decrease due to the evaporation process. Härtel, et al. [17] concludes that just a spray consisting of droplets with an diameter of 1 µm can saturate the air at any time liquid water is present.

Producing a fine and well distributed spray with mean droplet radii smaller than 5 µm for fast evaporation is technically challenging. To produce a spray with mean droplet diameter of 1 µm is technically rather impossible. Commonly used spray nozzles provide a spray with a mean diameter of about 30 µm. For the presented calculation a combination of a heat- and mass-transfer model for droplet evaporation and a thermodynamic model for the compression process calculation are investigated.

2.1 Compressor performance model

The calculation of compressor performance is realized by a simplified thermodynamic model for an adiabatic compressor. Acceleration and deceleration of the gas flow inside the compressor is neglected. Polytropic efficiency of the compressor is assumed to be

$$\eta_{poly} = \frac{v\,dp}{dh} = 0.9 \tag{3}$$

The compression rate C is set to

$$C = \frac{1}{p}\frac{dp}{dt} = 200\ s^{-1} \tag{4}$$

according to White, et al. [18]. This means that the pressure increases exponentially. Figure 2 shows calculated pressure and temperature trends of air according to the formula for dry compression.

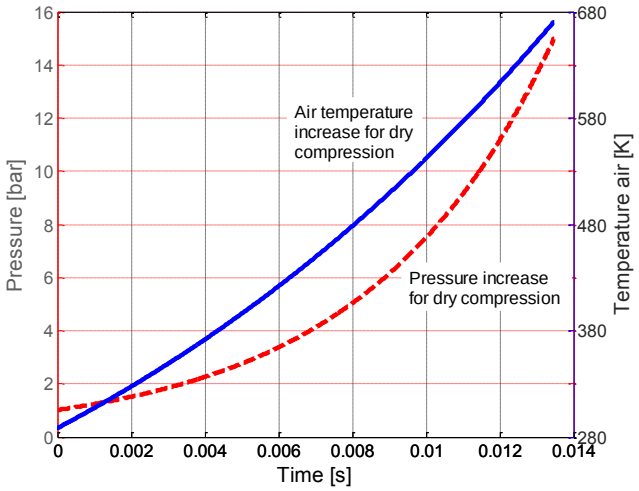

Figure 2 Pressure and air temperature trend for dry compression

For the calculations the same pressure increase is assumed for the dry and the wet compression process. Experimental and numerical studies reveal a stage mismatch and changed mass flow rate due to water injection for wet compression process see White, et al. [18] and Eisfeld, et al. [19]. These changed operating conditions lead to a minor pressure increase in the first compressor stages and a major pressure increase in the last compressor stages. The changed pressure increase influences the temperature rise due to the compression process. Irrespective of these changed operating conditions due to water injection is the pressure increase and dry air mass flow in the present study kept constant. This consideration affords to focus only on the water evaporation at identical conditions.

The temperature increase for the wet compression is determined in two steps. First the change of air temperature in

time step i due to the evaporation (indicated by superscript *) is computed using the energy balance:

$$\dot{m}^i_{air,dry} h^i_{air,dry} + \dot{m}^i_{vap} h^i_{vap} + \dot{m}^i_w h^i_w = \dot{m}^{i*}_{air,dry} h^{i*}_{air,dry} + \dot{m}^{i*}_{vap} h^{i*}_{vap} + \dot{m}^{i*}_w h^{i*}_w \quad (5)$$

$$\dot{m}^{i*}_{vap} = \dot{m}^i_{vap} + dm^i \quad (6)$$

$$\dot{m}^{i*}_w = \dot{m}^i_w - dm^i \quad (7)$$

$$T^{i*}_w = T^i_w + dT^i \quad (8)$$

dm_i denotes the evaporated mass flow which is estimated with the evaporation model. The water temperature change dT^i is also estimated using the evaporation model. Subsequent is the temperature increase due to compression process evaluated using the polytropic equation. The polytropic equation is formulated using the Gibbs-equation

$$Tds = dh - vdp \quad (9)$$

Inserting the polytropic efficiency

$$\frac{1}{\eta_{poly}} = \frac{dh}{v\,dp} \quad (10)$$

leads to

$$Tds = dh\,(1 - \frac{1}{\eta_{poly}}) \quad (11)$$

The real gas factor z of air for the regarded pressure and temperature range can be stated with $z \approx 1$ $(0.996 \leq z \leq 1.004)$. As a result it is reasonable to use the equations for ideal gas. Therefore, the specific volume is calculated with the formula $v = \frac{RT}{p}$. The enthalpy is expressed with the equation $dh = c_p dT$. This results in the known polytropic equation

$$T^{i+1}_{air} = T^{i*}_{air} \cdot \left(\frac{p^{i+1}_{air}}{p^i_{air}}\right)^{\frac{n-1}{n}} \quad (12)$$

The integration of Eq. 11 requires a further iteration step. Solving the problem by using the polytropic equation (Eq. 12) instead of the integration of Eq. 11 speeds the computation time up. The polytropic exponent n changes with vapor mass fraction in the air according to the change of κ.

$$\frac{n-1}{n} = \frac{1}{\eta_{poly}} \frac{\kappa - 1}{\kappa} \quad (13)$$

κ depends on pressure, air temperature and vapor mass fraction. The polytropic efficiency η_{poly} is kept constant. Figure 3 illustrates the scheme of the temperature calculation within the two steps.

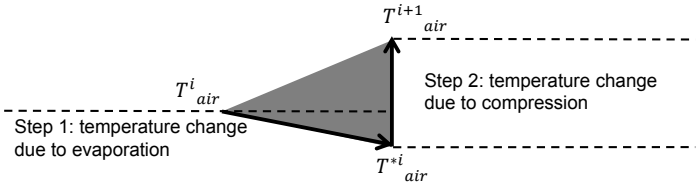

Figure 3 Scheme of temperature calculation

2.3 Droplet evaporation

The droplet evaporation model by Abramzon, et al. [14] (Abramzon-Sirignano model) is used to compute the evaporation process with a one-dimensional calculation tool. The following assumptions are used:

- Spherical droplets
- Monodisperse spray with mean diameter r_d
- Droplet breakup or conglomeration is neglected
- Wall interaction is neglected

The one-dimensional tool is well suited for a fast computational performance. The evaporation of one droplet with its characteristic diameter for the monodisperse spray is calculated. The droplet number of the spray is determined according to:

$$z_d = \frac{x_w \cdot m_{air,dry}}{\frac{4}{3}\,\pi\, r_d^3\, \rho_w} \quad (14)$$

with r_d as mean droplet diameter. For humid air, gas properties are taken from the property library by Kretzschmar, et al. [20]. Water properties according to IAPWS-IF97 tables are used from the property library by Kretzschmar, et al. [21]. The Abramzon-Sirignano model uses the extended film model to describe the droplet evaporation. The droplet vaporization rate is estimated with the formula

$$dm^i = 2\pi\, \bar{\rho_g}\, \overline{D_g}\, r_d\, Sh^* \ln(1 + B_M) \quad (15)$$

$\bar{\rho_g}$ and $\bar{D}_g$ are the average values of the gas film vapor density and of the diffusion coefficient. The average temperature and mass concentration of the gas film $\bar{T_g}$ and $\bar{Y_g}$ can be determined using the "1/3-rule" introduced by Yuen, et al. [22].

$$\bar{T_g} = T_w + \frac{1}{3}\,(T_{air} - T_w) \quad (16)$$

$$\bar{Y_g} = Y_{w,s} + \frac{1}{3}\,(Y_\infty - Y_{w,s}) \quad (17)$$

$Y_{w,s}$ is the vapor mass concentration at the film surface and Y_∞ is the vapor mass concentration far from the droplet. Figure 4 illustrates a droplet with film layer to clarify the definition of the vapor mass concentrations.

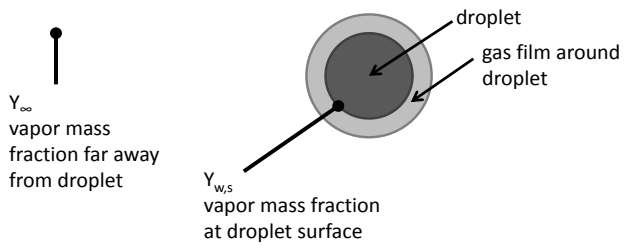

Figure 4 Scheme of water droplet with surrounding film layer and mass concentrations

The diffusion coefficient $\bar{D}_g$ in Eq. 15 is determined using the method given by Fuller, et al. [23]. Sherwood number Sh is the dimensionless mass transfer gradient at a surface. Ranz, et al. [24] gives a correlation for estimating the Sherwood number of a non-vaporizing droplet Sh_0, which is used here

$$Sh_0 = 2 + 0.552\, Re^{1/2}\, Sc^{1/3} \tag{18}$$

According to Abramzon, et al. [1] has the Sherwood-number of the non-vaporizing droplet Sh_0 to be modified to consider the convective mass transfer between droplet surface and gas environment using the Spalding mass transfer number B_M

$$Sh^* = 2 + \frac{(Sh_0 - 2)}{\frac{\ln(1+B_M)}{B_M}} \tag{19}$$

The Spalding mass transfer number B_M, an amount for the mass transfer between gas and liquid can be determined from the vapor mass fraction concentrations Y

$$B_M = \frac{Y_{w,s} - Y_\infty}{1 - Y_{w,s}} \tag{20}$$

The heat $\dot{Q}_L$ which is transferred into the liquid droplet is estimated using the formula by Abramzon, et al. [1]

$$\dot{Q}_L = \dot{m}\left\{\frac{\bar{c}_{p\,w,s}\,(T_{air} - T_w)}{B_T} - L(T_w)\right\} \tag{21}$$

The latent heat of evaporation $L(T_w)$ is calculated for the surface temperature of the droplet T_w. The radii of droplets used for interstage injection should be less than 5 µm. For such tiny droplets a uniform droplet temperature can be assumed. This leads to equilibrium of surface temperature of the droplet and the temperature at any point inside the droplet. With this assumption the droplet temperature can be exposed with the formula

$$\frac{dT_w}{dt} = \frac{\dot{Q}_L}{m_d c_{p,w}} \tag{22}$$

B_T is the Spalding heat transfer number according to the definition by Abramzon, et al. [14]

$$B_T = (1 + B_M)^{\phi} - 1 \tag{23}$$

with the non-dimensional correction parameter ϕ given by Abramzon, et al. [14]

$$\phi = \left(\frac{\bar{c}_{pw}}{\bar{c}_{pg}}\right)\left(\frac{Sh^*}{Nu^*}\right)\frac{1}{Le} \tag{24}$$

Correspondent to the Sherwood-number for mass transfer is the Nusselt-number the dimensionless temperature gradient at the droplet surface. The modified Nusselt-number is similarly to the modified Sherwood-number defined by Abramzon, et al. [1]:

$$Nu^* = 2 + \frac{(Nu_0 - 2)}{\frac{\ln(1+B_T)}{B_T}} \tag{25}$$

with Nu_0, the correlation for Nusselt-number of a non-vaporizing droplet, given by Ranz, et al. [24]:

$$Nu_0 = 2 + 0.552\, Re^{1/2}\, Pr^{1/3} \tag{26}$$

The assumption is made that droplets are injected into the gas mass flow with the droplet velocity $\mathrm{u_d} = 160\ \mathrm{ms^{-1}}$. The air velocity during the compression process is set constant to $\mathrm{u_\infty} = 175\ \mathrm{ms^{-1}}$ corresponding to typical axial-compressor specifications. According to Abramzon, et al. [1] can the change of the droplet velocity be evaluated by the formula

$$\frac{du_d}{dt} = \frac{3\,C_D}{2\,r_d}\left(\frac{\rho_\infty}{\rho_w}\right)|u_\infty - u_d\,|(u_\infty - u_d\,) \tag{27}$$

The drag coefficient C_D is defined by Faeth [25]

$$C_D = \frac{24}{Re}\left[1 + \frac{Re^{2/3}}{6}\right] \tag{28}$$

The relative velocity between gas phase and droplet influences the evaporation performance. The relative velocity $u_{rel} = |u_d - u_\infty|$ between gas and droplet is used to determine the Reynolds-number Re of the droplet. This Reynolds-number is used for the droplets Sherwood-number Sh_0 (Eq.18) and Nusselt-number Nu_0 (Eq. 26). A one-dimensional approach incorporates of cause a one dimensional relative velocity. Considering the droplets acceleration and deceleration in relation to the air the relative velocity vector transfers this into a one-dimensional scheme and enables the usage of a one-dimensional evaporation model.

Table 1 Basic conditions for determination of velocity change for water injected into compressor flow

Property	
Air velocity (constant)	175 ms^{-1}
Droplet velocity at injection point	160 ms^{-1}
Air temperature	288.15 K
Water temperature	288.15 K
Air pressure	1 bar
Droplet radii	2 µm, 5 µm
Droplet Reynolds-number	26325, 65711
Droplet Weber-number	0.006, 0.015

Inside the compressor, a uniform air velocity of 175 ms^{-1} is assumed. To validate the small droplets ability to follow the main gas flow a previous study is performed. Droplets with initial radii of 2 µm and 5 µm are selected for the pre-study. The relative velocity between gas phase and droplets is set to

15 ms^{-1}. In this case amounts the relaxing time for droplets with an initial radius of 2 µm to 0.05 ms. 5 µm droplets reach 0.4 ms after injection the gas velocity, see Fig. 5.

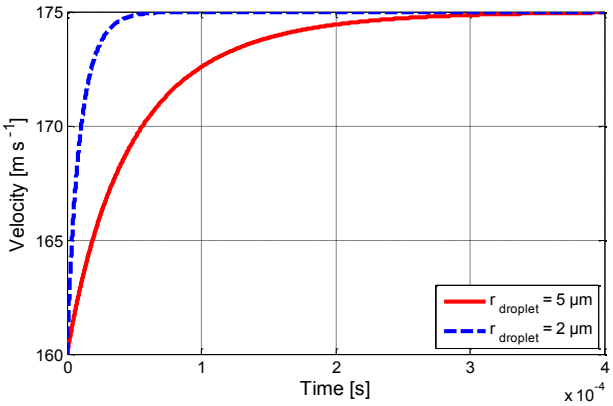

Figure 5 Velocity of droplets injected into compressor air mass flow, relative velocity $u_{rel} = 15\ ms^{-1}$

The size of droplets used in the present calculations is so small that the three dimensional character of the compressor flow is neglected due to the fact that the acceleration process of these small droplets is very fast. No slip velocity condition is used for the presented study.

2.4 Comparison of droplet evaporation models

Kim, et al. [26] and Kim, et al. [10] estimate the droplet evaporation for a technical analysis of the wet compression process with two different evaporation models. In the first publication Kim, et al. [26] uses the droplet evaporation model by Spalding. Within the second publication (Kim, et al. [10]) the analytical non-equilibrium solution is used to compute the wet compression process. For both calculations the pressure rise inside the compressor is determined with Eq. (4) according to White, et al. [18]. The compressor specifications are:

- compression rate $C = 200\,\frac{1}{s}$
- pressure ratio $\pi = 15$
- polytropic compressor efficiency $\eta_{poly} = 90\%$
- ISO-conditions for the air at compressor inlet

In the presented calculation the same compressor model and the same ISO conditions of the air are used. As mentioned in chapter 2.3 no slip velocity condition is assumed. All three models show different evaporation performances for the same compression process, see Fig. 6. The Abramzon-Sirignano model calculates a slower evaporation performance compared to the two other models. The difference in the evaporation time between the Spalding model and the Abramzon-Sirignano model is about 0.002 s for a 2 µm droplet. The same evaporation level of the 4 µm droplet is calculated with a time delay of about 0.0023 s with the Abramzon-Sirignano model compared to the Spalding model [25]. The spray consisting of 4 µm droplets is not completely evaporated when the compression process is finished. The evaporation process calculated with the Abramzon-Sirignano model for a spray consisting of droplets with an initial diameter of 5 µm is still not finished when the compression process is finished. The non-equilibrium assumption shows a complete evaporation of the 5 µm droplets 0.005 s before the end of the compression process.

The evaporation trend of the 2 µm and the 4 µm droplets by the Abramzon-Sirignano model and by the Spalding model are similar. In contrast to the Abramzon-Sirignano model the evaporation trend of the non-equilibrium model differs significantly, see Fig. 6. It has to be considered that different evaporation models result in different evaporation performances at compressor conditions. Because of the lack of experimental data no thorough validation of the evaporation models is available. In the presented calculations the Abramzon-Sirignano model is used because of its good acceptance in the research community.

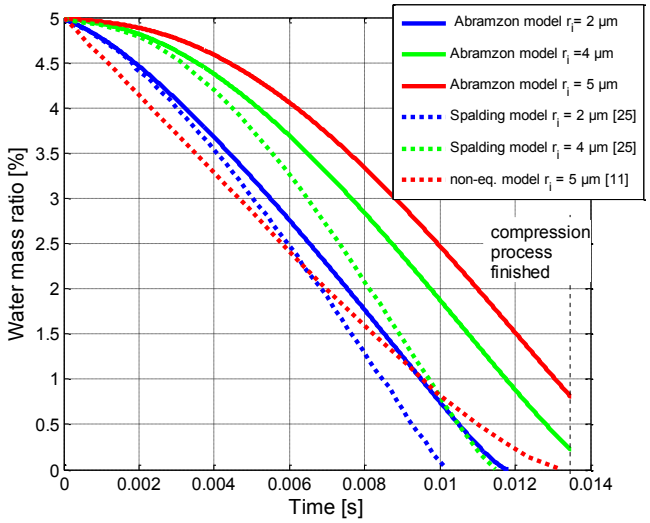

Figure 6 Droplet evaporation performance calculated with C=200 s^{-1}, π=15, η_{poly}=90%, air ISO conditions at compressor inlet, water mass fraction x_w= 5%

3. Results and discussion

The evaporation performance in a compressor depends mainly on three factors

- Relative velocity between gas and liquid
- Droplet radius
- Temperature difference between gas and liquid

The relevance of the relative velocity between gas and droplet is not apprenticed if the droplet radius goes below the target value of 5 µm. Consequently this examination disregards the impact of the relative velocity on the evaporation performance. The analysis how the droplet radius and the temperature difference between gas and liquid impacts the evaporation performance can give an indication how the evaporation process for compressor cooling can be optimized. For all calculations it is postulated that air enters the compressor at ISO conditions. Basic conditions for the calculations are given in Tab. 2.

Table 2 Basic conditions for calculations

Property	
Air temperature compressor inlet	288.15 K
Air pressure compressor inlet	1 bar
Air humidity (relative)	60 %
Water temperature injection point	288.15 K
Pressure ratio π	15
Compression rate C	$200 s^{-1}$

3.1 Droplet radii and water mass fraction

The droplet radius is one of the main factors influencing the evaporation performance of droplets. Spalding [27] gives the correlation, that the square of the droplet diameter decreases linear with time. This assumption fits well for droplets in resting air and at ambient conditions. In the present study, the droplets are injected in an air mass flow with changing conditions due to compression and evaporation process. The relation between droplet volume and droplet surface is important for the present study. Decreasing the droplet diameter increases the ratio of droplet surface to droplet volume.

In Tab. 3 is the evaporation time in dependence of droplet radius and water mass fraction listed. The basic conditions from Tab. 2 are used for the calculations. The initial droplet radii are 1 µm, 2 µm, 3 µm, 4 µm and 5 µm respectively. A decreasing droplet radius decreases the evaporation time of the droplet. Consequently decreases the evaporation time with decreasing water mass ratio. Also a higher water mass ratio leads to a higher vapor mass fraction in the air during the evaporation process. The Spalding mass transfer number B_M is an indicator for the mass transfer between the droplets and the surrounding gas. In Fig. 7 is the Spalding mass transfer number B_M in dependence of the evaporation time pictured. The calculations are made for a spray, consisting of droplets with an initial diameter of 1 µm but different water mass fractions. The mass transfer number refers to the ratio between vapor mass fraction in the air and at the droplet surface. The difference between the vapor mass fraction at the droplet surface and in the gas mass flow away from the droplet increases with decreasing water mass ratio. Hence B_M gets higher if less water is injected and this leads to a faster evaporation process.

Table 3 Evaporation time in dependence on droplet radius and water mass fraction

Radius [µm]	x_w=5% evap. time [s]	x_w=4% evap. time [s]	x_w=3% evap. time [s]	x_w=2% evap. time [s]	x_w=1% evap. time [s]
5	n.evap.	n.evap.	n.evap.	0,013	0,012
4	n.evap.	n.evap.	0,012	0,011	0,010
3	0,013	0,012	0,010	0,009	0,008
2	0,012	0,010	0,009	0,007	0,006
1	0,011	0,009	0,007	0,005	0,004

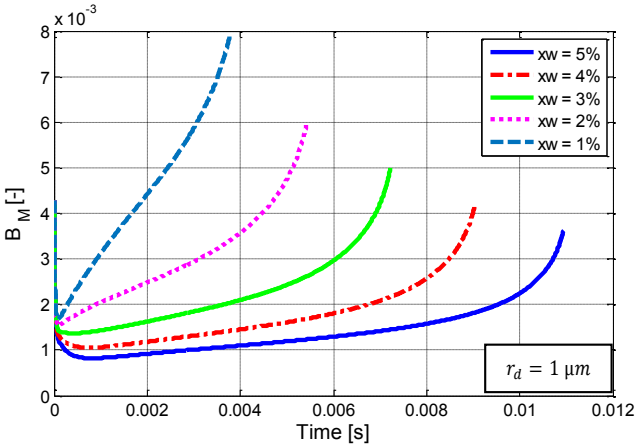

Figure 7 Dependency of Spalding number of mass transfer B_M on water mass ratio x_w and evaporation time for a spray with an initial droplet radius of 1 µm

For the same droplet radius results an increased water mass ratio in an augmented number of water droplets. The augmented number of droplets causes a slower evaporation process of a single droplet. The slower evaporation follows from the enlarged vapor mass in surrounding according to the numerous evaporating droplets.

Figure 8 shows the air temperature degradation due to the water evaporation within 0.004 s during the compression process. Different water mass fractions as well as different spray droplet radii are regarded. As demonstrated before a water mass fraction of 1 % consisting of 1 µm droplets evaporates within 0.004 s. The depicted temperature drop of 35.39 K is the maximum temperature drop which can be reached with this configuration. Besides, the temperature drop raises in consequence of the spray evaporation with an increasing water mass fraction but unchanged droplet radius. The maximum temperature decrease ($\Delta T = 52.94\ K$) can be reached with an injected water mass fraction of 5 % and a spray consisting of droplets with an initial radius of 1 µm. As expected, leads a smaller water mass fraction with same droplet radii in the regarded time to a minor evaporative air cooling effect than a higher amount of injected water.

Furthermore, the cooling effect diminishes if the droplet radius increases but the water mass fraction is kept constant. The trend is irrespective of the analyzed water mass fractions of 1 % to 5 %. Thus, the strength of the temperature drop depends on the droplet radius. The evaporation rate is substantial for the cooling effect within the short period of 0.004 s. A water mass fraction of 1 % and a spray consisting of 1 µm droplets leads to an air temperature drop of 35.39 K whereas a water mass fraction of 3 % und a spray consisting of 2 µm droplets leads to an air temperature drop of 36.11 K. The difference is only 0.72 K. It is worth mentioning that in this case a higher water mass fraction with increased droplet radius leads to a slightly better cooling effect though the evaporation of the single droplets performs slower. Even within one diameter class enhances the cooling effect with an enlarged water mass fraction.

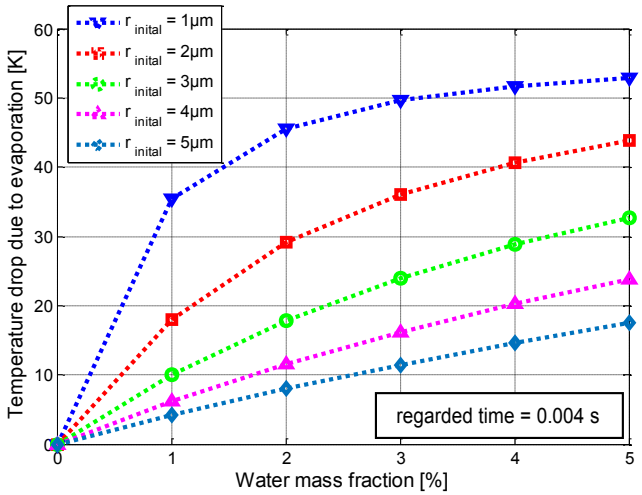

Figure 8 Temperature decrease for different droplet radii and water mass fractions, evaporation time = 0.004 s

The decelerated evaporation performance of a single droplet due to the exceeded vapor mass fraction in the air is less significant than the cooling effect introduced by the evaporation of the huge number of droplets in the spray. Therefore, the cooling effect of a higher amount of injected water with the same droplet radius is more substantial than the evaporation effect of a small water mass ratio. Though a substantial augmented droplet radius but same water mass fraction leads to a declining evaporation performance and therefore a declining air temperature drop. Air is heated up at $T_{air} = 371.45\ K$ due to the compression process if no water is injected. The injection of 5 % water mass fraction consisting of droplets with an initial radius of 1 µm decreases the air temperature by about $\Delta T = 52.9\ K$. For the same mass fraction but droplets with an initial radius of 5 µm is the air temperature decreased by about $\Delta T = 17.5\ K$. It can be pointed out that both, water mass fraction and droplet radii, have a significant influence on the cooling performance of compressed air.

3.2 Temperature difference between gas and liquid

Increasing the water temperature leads to a reduction of water surface tension which results in an enlarged Weber-number. Spray generation at enlarged Weber-numbers results in reduced droplet diameter. The evaporation performance for two exemplary water temperatures is presented in this study. The lower water temperature is set to 293.15 K, the higher water temperature is set to 353.15 K. This temperature increase leads to a decrease of the surface tension about 16 %. Weber-number for atomizers is defined as

$$We = \frac{d\, u^2\, \rho}{\sigma} \tag{29}$$

Fluid velocity u and the nozzle diameter d are kept constant for both cases. The ratio of the Weber-number at 293.15 K to the Weber-number at 353.15 K is therefore estimated to

$$\frac{We_{T_w=293.15K}}{We_{T_w=353.15K}} = \frac{\sigma_{T_w=353.15K}\ \rho_{T_w=293.15K}}{\sigma_{T_w293.15K}\ \rho_{T_w=353.15K}} = 88.5\%$$

This means a rise of Weber-number about 11.5 % for a water temperature increase of $\Delta T_w = 60K$. Also a slight augmentation of water temperature has a positive effect on the generation of small droplets. Furthermore a spray consisting of small droplets leads to an improved air cooling effect.

Besides the effect of increased water temperature on the evaporation performance has to be considered. In Fig. 9 the water temperature reduction for initial droplet radii of 2 µm, 5 µm and 10 µm, injected with an initial water temperature $T_w = 353.15\ K$ is pictured. Basic conditions, mentioned in Tab. 2 are used for the determination of the evaporation performance.

The droplet temperature decreases faster with diminishing droplet diameter. The air temperature at the beginning of the calculation is set to 288.15 K. The temperature of a droplet with a radius of 2 µm declines within 0.0003 s from 353.15 K to air temperature level. For a droplet with an initial radius of 5 µm the water temperature decreases due to convection and latent heat of vaporization within 0.001 s. Consequential drops the temperature of the 10 µm droplet slower than the temperature of the droplets with 2 µm and 5 µm.

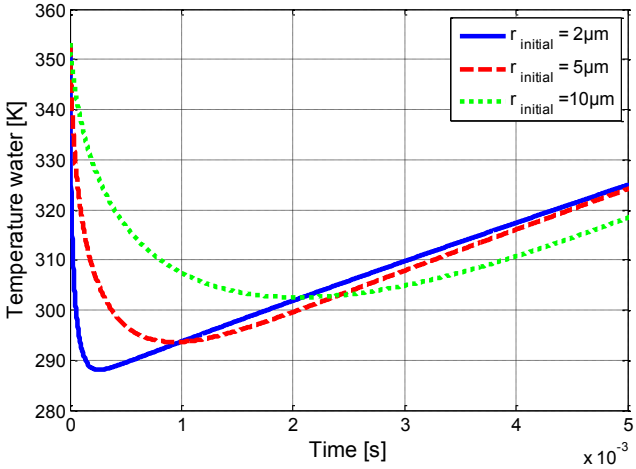

Figure 9 Decrease of water temperature for different initial droplet radii

Figure 10 depicts the influence of the water temperature on the evaporation time of the generated droplets. The spray mass flow is set to 2 %. The initial droplet radius is set to $r_d = 2\ \mu m$. The initial water temperature for the first case is set to 293.15 K. For the second case is the initial water temperature set to 353.15 K. As mentioned before, the droplets injected with an initial temperature of 353.15 K reach air temperature level within 0.0003 s. It can be shown that within these 0.0003 seconds the evaporation rate is slightly higher than the evaporation rate of the spray with minor initial water temperature. The droplet radius for an initial water temperature of 353.15 K decreases by 4 %. The radius of a droplet injected at 293.15 K decreases in the same time by 0.5 %. After that period the evaporation performance of both sprays is comparable. The initial offset due to faster evaporation of the spray injected at higher initial water temperature is almost constant for the whole evaporation process. Just a small advantage in the evaporation performance due to a rise of water temperature can be observed.

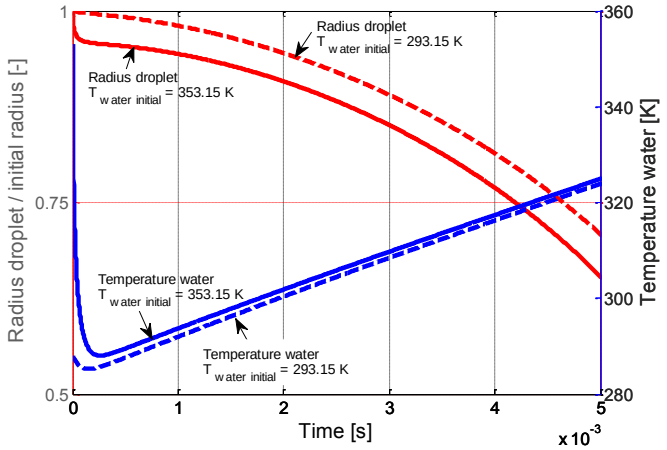

Figure 10 Droplet evaporation and water temperature change for a spray with initial radius r=2 µm and initial water temperature of 293.15 K and 353.15 K

3.3 Multiple water injection during the compression process

The last section of this paper deals with the evaporative cooling of the compressed air by multiple water injection during the compression process. Due to the fact that droplets with a small initial radius evaporate faster than droplets with a bigger radius, computations are realized for a spray consisting of droplets with an initial radius of 1 µm. Three case studies are performed. The sequenced injection of 1 % water mass fraction at six positions is analyzed in case 1. In case 2 the injection of 2 % water mass fraction injected at three sequenced positions is examined. The third case focuses on the injection of 6 % water mass fraction at once at the compressor inlet. The sum of the injected water mass fraction in all three cases amounts to 6 % of the dry air mass flow. The results of the different water injection strategies are shown in Fig. 11.

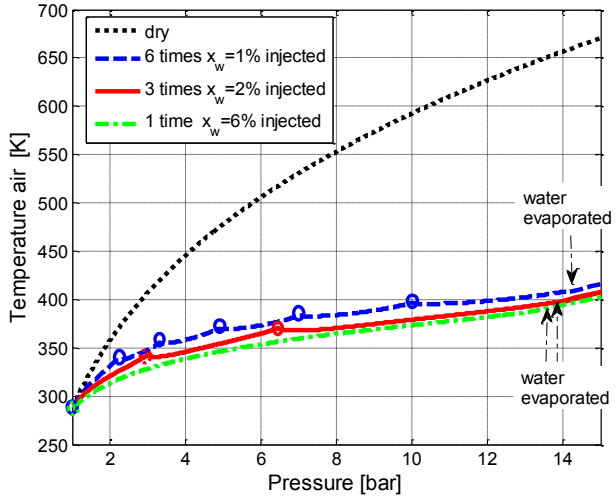

Figure 11 Temperature air for compression process with multiple water injection

The injection positions are marked with circles. The black line pictures the dry compression process without any water injection as reference. The blue line illustrates the air temperature for case 1 (1 % water injection at six positions); the red line depicts the air temperature for the second case (2 % water injection at tree positions) and the green line depicts the air temperature for case 3 (6 % water injection at one single position).

Table 4 Temperature decrease due to multiple water injection

Water mass fraction x_w [%]	Temperature at compressor outlet [K]	Temperature decrease due to evaporative cooling [K]
0	673.2	0
6 times 1 %	416.0	257.2
3 times 2 %	408.5	264.7
1 time 6 %	402.7	270.5

In all three cases the whole amount of injected water evaporates before the compression process is finished (the particular positions are marked with arrows). The amount of 6 % water mass fraction evaporates slightly faster, if the entire water is injected at once (case 3). For the slower evaporation performance of the cases with multiple injections (case 1 and case 2) one effect is responsible: In every calculation and at every injection position the water injected is at 288.15 K. The later the water is injected the higher the temperature difference is between the injected droplets and the gas phase. Additionally the vapor mass fraction in the air is higher if the water is injected in further stages. Vapor from the heated gas phase condenses at the cold droplet surface until the water temperature exceeds the specific dew point temperature. The droplet radius increases due to the added mass. The droplet radius augmentation increases with a higher vapor mass fraction in the gas phase and a greater temperature difference between liquid and gas. The radius of the droplets injected at position six for case 3 for example augments about 4 %. The increased droplet radius results in a slower evaporation performance. The condensation results in a reduced cooling effect.

The air temperature at the compressor outlet decreases in all three cases about 260-270 K due to the injection of 6 % water mass fraction. Numerous injections with smaller water amounts each (case 1) lead to a slightly higher outlet temperature of 7.5 K than fewer injections (case 2) with the same overall water amount but higher water amounts at each injection position. The difference between six continuous water injections and one primary water injection (case 1) is 13.3 K. The difference of the temperature rise depends also on the variation of the polytropic coefficient due to the evaporation rate. A higher amount of water vapor in the gas phase leads to decreasing polytropic coefficients. For smaller polytropic coefficients the air temperature increases more significantly due to the compression process (see Eq. 9).

In the presented investigation droplet deposition due to droplet-wall interactions is neglected. With this assumption the calculated evaporation rate surpasses the technically feasible rate because of the smaller evaporation rate of water films compared to droplet evaporation.

Although small droplets follow the main flow best, it is not possible to avoid a contact between droplets and walls completely. The risk of droplet deposition on walls increases with higher amounts of injected water. Smaller amounts of

water during a single injection decrease the droplet deposition. Simultaneously the risk of blade erosion due to droplet impact decreases. Hence the injection of smaller amounts of water at numerous positons is preferable to higher amounts injected at one single position. The distinct evaporative cooling leads to reduced power consumption of the compression process. The higher mass amount due to water injection increases the mass flow and therefore the turbine workload in a gas turbine cycle. One disadvantage of a decreased compressor outlet temperature is the need of higher fuel mass to reach the requested turbine inlet temperature. An analysis of the whole gas turbine cycle is necessary for a clear statement as to which effect predominates.

4. Conclusion

This contribution deals with spray evaporation during a compression process in an axial compressor. The influence of the injected water mass and the droplet radius is demonstrated. As expected, a smaller droplet radius results in faster evaporation. This leads to a stronger decrease of air temperature when the same water amount with smaller droplets is injected. Increasing the water mass for a spray consisting of droplets of the same diameter decelerates the evaporation process. An elevated initial droplet temperature results in a minor positive effect on the evaporation performance but in higher Weber-numbers and therefore smaller droplets for the same nozzle configuration.

Water injection during the compression process decreases the air temperature continuously. Injection of a spray consisting of tiny droplets with a radius $r_d = 1\,\mu m$ at different positions into the compressor allows a strong decrease of the compressor outlet temperature. In the investigated cases a water mass fraction of 6 % is injected. This leads to a compressor outlet temperature decrease about 65 %. The injection of higher water amounts at fewer positions leads to a slightly stronger temperature drop at the compressor outlet than the water injection at numerous positions.

The application of different evaporation models results in varying evaporation performances. For further investigation of the evaporation during the compression process a detailed comparison of the evaporation model performances should be executed. Correspondent to the comparison the model which reproduces the influence of high temperature and high pressure conditions on the evaporation process in the best way should be chosen. The present approach neglects changes in the compressor performance due to the water injection. Future precise calculations should take into consideration that water injection may lead to stage mismatching and therefore to a changed compressor performance.

5. References

[1] B. Abramzon and W. Sirignano. Droplet vaporization model for spray combustion calculations. *Int J Heat and Mass Transfer.* 32(9): 1605–1618, 1989.

[2] M. Chaker; C. B. Meher-Homji; T. Mee. Inlet Fogging of Gas Turbine Engines—Part I: Fog Droplet Thermodynamics, Heat Transfer, and Practical Considerations. *J Eng Gas Turb Power.* 126(3): 545, 2004.

[3] Q. Zheng; Y. Sun; S. Li; Y. Wang. Thermodynamic Analyses of Wet Compression Process in the Compressor of Gas Turbine. *J Turbomach.* 125(3): 489, 2003.

[4] Q. Zheng; M. Li; Y. Sun. Thermodynamic Performance of Wet Compression and Regenerative (WCR) Gas Turbine. *Proc. ASME Turbo Expo 2003,* 813–820, 2003.

[5] M. Bianchi; F. Melino; A. Peretto; P. R. Spina; S. Ingistov. Influence of Water Droplet Size and Temperature on Wet Compression. *Proc. ASME Turbo Expo 2007,* GT2007-27458, 2007.

[6] K. Brun; R. Kurz; H. R. Simmons. Aerodynamic Instability and Life-Limiting Effects of Inlet and Interstage Water Injection Into Gas Turbines. *J Eng Gas Turb Power.* 128(3): 617, 2006.

[7] L. Sun. Numerical Simulation of a Complete Gas Turbine Engine With Wet Compression. *J Eng Gas Turb Power.* 135(1): 1–12, 2013.

[8] J. Wang; Q. Zheng; L. Sun; M. Luo. The Effective Positions to Inject Water Into the Cascade of Compressor. *Proc. ASME Turbo Expo 2012.* GT2012-69158, 2012.

[9] M. Bagnoli; M. Bianchi; F. Melino; A. Peretto; P. R. Spina; R. Bhargava; S. Ingistov. A Parametric Study of Interstage Injection on GE Frame 7EA Gas Turbine. *Proc. ASME Turbo Expo 2004,* 489–499, 2004.

[10] K. H. Kim; H.-J. Ko; H. Perez-Blanco. Analytical modeling of wet compression of gas turbine systems. *Appl Thermal Engineering.* 31(5): 834–840, 2011.

[11] I. Roumeliotis and K. Mathioudakis. Evaluation of Interstage Water Injection Effect on Compressor and Engine Performance. *J Eng Gas Turb Power.* 128(4): 849–856, 2006.

[12] S. Ingistov. Interstage Injection System for Heavy Duty Industrial Gas Turbine Model 7EA. *Proc. ASME Turbo Expo 2001, 2001-GT-0407,* 2001.

[13] J. P. Schnitzler; I. von Deschwanden; F.-K. Benra; H. J. Dohmen. Experimental Determination of a Four Stage Axial Compressor Map Operating in Wet Compression. *Proc. ASME Turbo Expo 2014, GT2014-26807,* 2014.

[14] B. Abramzon and W. Sirignano. Approximate theory of a single droplet vaporization in a convective field: effects of variable properties, Stefan flow and transient liquid heating. *Proc. 2nd ASME-JSME Thermal Eng. Joint conf (*1): 11–18, 1987.

[15] A. J. White and A. J. Meacock. An Evaluation of the Effects of Water Injection on Compressor Performance. *J Eng Gas Turb Power.* 126(4): 748, 2004.

[16] J. Young. The fundamental equations of gas-droplet multiphase flow. *Int J Multiphase Flow.* 21(2): 175–191, 1995.

[17] C. Härtel and P. Pfeiffer. Model Analysis of High-Fogging Effects on the Work of Compression. *Proc. ASME Turbo Expo 2003,* 689–698, 2003

[18] A. J. White and A. J. Meacock. An Evaluation of the Effects of Water Injection on Compressor Performance. *Proc. ASME Turbo Expo 2003*, 2003.

[19] T. Eisfeld, F. Joos Experimental Investigation of the Aerodynamic Performance of a Linear Axial Compressor Cascade With Water Droplet Loading. *Proc. ASME Turbo Expo 2010*, GT2010-22831, 2010.

[20] H.-J. Kretzschmar; I. Stoecker; M. Kunick; K. Knobloch; T. Hellriegel; L. Kleemann; D. Seibt. Property Library for Humid Air Calculated as Ideal Mixture of Real Fluids.

[21] H.-J. Kretzschmar; I. Stoecker; M. Kunick; S. Herrmann. Property Library for the Industrial Formulation IAPWS-IF97 for Water and Steam.

[22] M. C. Yuen and L. W. Chen. On Drag of Evaporating Liquid Droplets. *Comb Science and Technology.* 14(4-6): 147–154, 1976.

[23] E. N. Fuller; P. D. Schettler; J. C. Giddings. New Method for Prediction of Binary Gas-Phase Diffusion Coefficients. *Industrial & Engineering Chemistry.* 58(5): 18–27, 1966.

[24] W. E. Ranz and W. R. Marshall. Evaporation from drops Part II. *Chem. Eng. Progr.* 48(4): 173–180, 1952.

[25] G. M. Faeth. Current status of droplet and liquid combustion. *Progress in Energy and Combustion Science.* 3(4): 191–224, 1977.

[26] K. H. Kim and H. Perez-Blanco. An Assessment of High-Fogging Potential for Enhanced Compressor Performance, *Proceedings of ASME Turbo Expo 2006,* GT2006-90482, 2006.

[27] D. B. Spalding. The combustion of liquid fuels. *Symposium (International) on Combustion.* 4(1): 847–864, 1953.